Double-templated electrodeposition: Simple fabrication of micro-nano hybrid structure by electrodeposition for efficient boiling heat transfer

Cite as: Appl. Phys. Lett. **101**, 251909 (2012); https://doi.org/10.1063/1.4772539
Submitted: 01 October 2012 . Accepted: 29 November 2012 . Published Online: 20 December 2012

Sangwoo Shin, Beom Seok Kim, Geehong Choi, Hwanseong Lee, and Hyung Hee Cho

Double-templated electrodeposition: Simple fabrication of micro-nano hybrid structure by electrodeposition for efficient boiling heat transfer

Sangwoo Shin, Beom Seok Kim, Geehong Choi, Hwanseong Lee, and Hyung Hee Cho[a)]
Department of Mechanical Engineering, Yonsei University, Seoul 120-749, South Korea

(Received 1 October 2012; accepted 29 November 2012; published online 20 December 2012)

Micro-nano hybrid structure (MNHS) that comprises of microcavities and nanowires is a specific class of MNHS that is considered to be ideal for two-phase boiling heat transfer applications. Realizing MNHS with electrodeposition is favorable in boiling heat transfer, but the realization has been very difficult and time-consuming to achieve. Here, we demonstrate a simple, robust, rapid, and photolithography-free route to fabricate MNHS that consists of individual microcavities and copper nanowires on a large area. We show that this MNHS can be extremely beneficial in boiling heat transfer compared to the state-of-the-art nanowire surface. © *2012 American Institute of Physics*. [http://dx.doi.org/10.1063/1.4772539]

Cooling technology holds a key promise to the ever-increasing integration density in microelectronics industries where the excess heat dissipation in hotspots must be removed by vigorous cooling technologies.[1] To this end, two-phase heat transfer methods such as condensation,[2] evaporation,[3] and boiling[4,5] are once again gaining their interest. Above all, boiling heat transfer is not only a promising cooling scheme for microelectronics but also is important in wide range of technical applications that involves cooling of hot components in macro- as well as microscale devices because of its efficient cooling mechanism. To date, vast effort has been devoted to enhancing the boiling heat transfer performance mostly by modifying the surface characteristics in terms of surface wettability and surface morphology because these are the most dominant factors that determine the boiling heat transfer performance such as critical heat flux (CHF), heat transfer coefficient (HTC), and onset of nucleation boiling (ONB).

Recently, with aid of nanotechnology, researchers have revealed that nanostructures, especially nanowires, can be extremely beneficial to boiling heat transfer, and this has once again provoked the boiling heat transfer community for further research.[4–9] The nanowires employed in this specific application requires densely distributed nanowires with large aspect ratio that accommodates high surface wettability, large capillary pumping, as well as enlarged surface area.[4] This class of nanowires can be easily synthesized by electrochemical routes such as metal-assisted electrochemical etching method[4,6,8–11] and template-assisted electrochemical deposition method.[4,6,12,13] The former method, metal-assisted electrochemical etching, is extremely simple and robust. However, this method can only be applied to certain materials, mostly silicon.[14] Critical fact is that the silicon nanowires fabricated by this method exhibit extremely low thermal conductivity compared to bulk because of the rough surface morphology that favors phonon boundary scattering. This leads to about two orders of reduction in thermal conductivity that nearly reaches so-called "amorphous limit."[15]

The latter method, template-assisted electrochemical deposition method, is relatively complex because additional features such as template, electrodes, and power supply are accompanied. Nonetheless, the choice of materials are almost limitless for conductive materials and the surface morphology can be easily tailored, which makes the template-assisted electrochemical deposition most attractive method in realizing nanowire surface for boiling heat transfer. Highly dense copper nanowires with aspect ratio for over 100 can be easily realized with this method, which leads to dramatic enhancement in boiling heat transfer performance.[4,6]

Many recent reports on enhancing boiling heat transfer via electrochemically synthesized nanowires attribute to enlarged nucleation cavity sites that are formed by natural agglomeration of nanowires during drying of the wet chemicals.[4,6,8,9] However, such cavities are spontaneously formed where the location, size, and shape of the cavities are highly random and dispersed. Also, these cavities are not fully robust and intact to endure the violent bubbling at high heat flux regime.

In this regard, a micro-nano hybrid structure (MNHS) that comprises of microcavities and nanowires should be an ideal surface for boiling heat transfer because the artificial microcavities of dimensions in several tens of microns can act as a robust nucleation sites, while the densely distributed nanowires can provide capillary pumping and wettability. However, fabricating MNHS involves relatively time-consuming fabrication processes. Especially, in order to fabricate MNHS by template-assisted electrodeposition, photolithography process is inevitable for microstructure patterning because imprinting or sub-10 μm shadow mask is practically unfeasible.[16] However, direct patterning of photoresist on top of the rough porous membrane is nearly impossible because photoresists can easily penetrate into the hydrophilic membrane, or unevenly coat because of high surface roughness.[17] Therefore, with the need of simpler fabrication method that does not require photolithography process for fabricating micro-nano hybrid structure, we propose a simple and rapid route to achieve MNHS by so-called "double templating." By using two different porous membranes that differ from pore size and density, namely, anodic

[a)]Author to whom correspondence should be addressed. Electronic mail: hhcho@yonsei.ac.kr.

aluminum oxide (AAO) and polycarbonate track-etch (PCTE) membranes, a rapid fabrication of electrodeposited MNHS can be obtained on a large area. We demonstrate that this surface can be an ideal surface for boiling heat transfer due to the artificially created microcavities that act as nucleation sites. While most studies focus on enhancing CHF, we report a prominent enhancement of HTC and ONB by electrodeposited MNHS surface. Even compared to the nanowire-only surface, 45% of HTC enhancement and 49% of wall superheat reduction at ONB are achieved. Since CHF can be thought as a cooling "capacity," whereas HTC can be thought as a cooling "efficiency," and also ONB can be regarded as "easiness" of nucleate boiling to occur, which is in accordance with efficiency, we claim that the proposed MNHS surface can be viewed as a highly efficient boiling surface.

A schematic of the process for the fabrication of electrodeposited MNHS is presented in Figure 1. Detailed procedures for boiling heat transfer experiment can be found in the supplementary information.[18] Two different porous membranes are employed in which AAO is mounted on top of the copper seed layer, followed by PCTE membrane (Figures 1(b) and 1(c)). Compared to AAO, PCTE membrane exhibits wide range of pore sizes, ranging from several nanometers to tens of microns, and the pore size is well-defined and homogeneous. Also, the pore density of PCTE is relatively lower by few orders compared to AAO. These facts lead to the idea that PCTE can serve as an excellent shadow mask for sub-10 μm features that can be employed to pattern the microstructures for MNHS. Therefore, we sputtered 400 nm of copper mask film on the surface of the 10 μm pore sized PCTE membrane that was located on top of the AAO membrane. Subsequently, the upper PCTE membrane was removed, forming a microscopic copper mask islands on top of the AAO membrane (Figures 1(d) and 1(e)). This microisland-masked AAO membrane was directly employed as a template for copper nanowires, which will eventually form numerous microscale cavities along the nanowire surface. The copper nanowires were grown directly on the surface of copper-coated silicon substrate to minimize the thermal boundary resistance between the nanowires and the substrate.[6] After electrodeposition, the AAO membrane was completely dissolved in order to form MNHS.

A clear formation of circular microcavities within the forest of copper nanowires can be identified in Figures 1(f) and 1(g). Along with artificially formed circular microcavities, narrow crevice-like microcavities are also randomly formed by spontaneous agglomeration of nanowires. To date, as mentioned earlier that these naturally formed cavities are regarded as one of the major factors that contribute to the boiling enhancement via nanowires.[4,6,8,9] However, these microcavities are formed in a random fashion with low robustness. Moreover, such long and narrow geometries are not the most favorable one for nucleating and releasing bubbles. Rather, a circular shaped cavity should be favorable for growing, maintaining, and releasing the bubble with minimum Helmholtz free energy.[19] Thus, these artificially formed circular microcavities can be expected to benefit boiling heat transfer.

Moreover, we observed that the contact angle of MNHS was nearly zero, and this superhydrophilic surface characteristic of MNHS surface should be favorable for promoting additional capillary pumping to the boiling sites thereby extending CHF.[4,6] Therefore regarding these advantageous

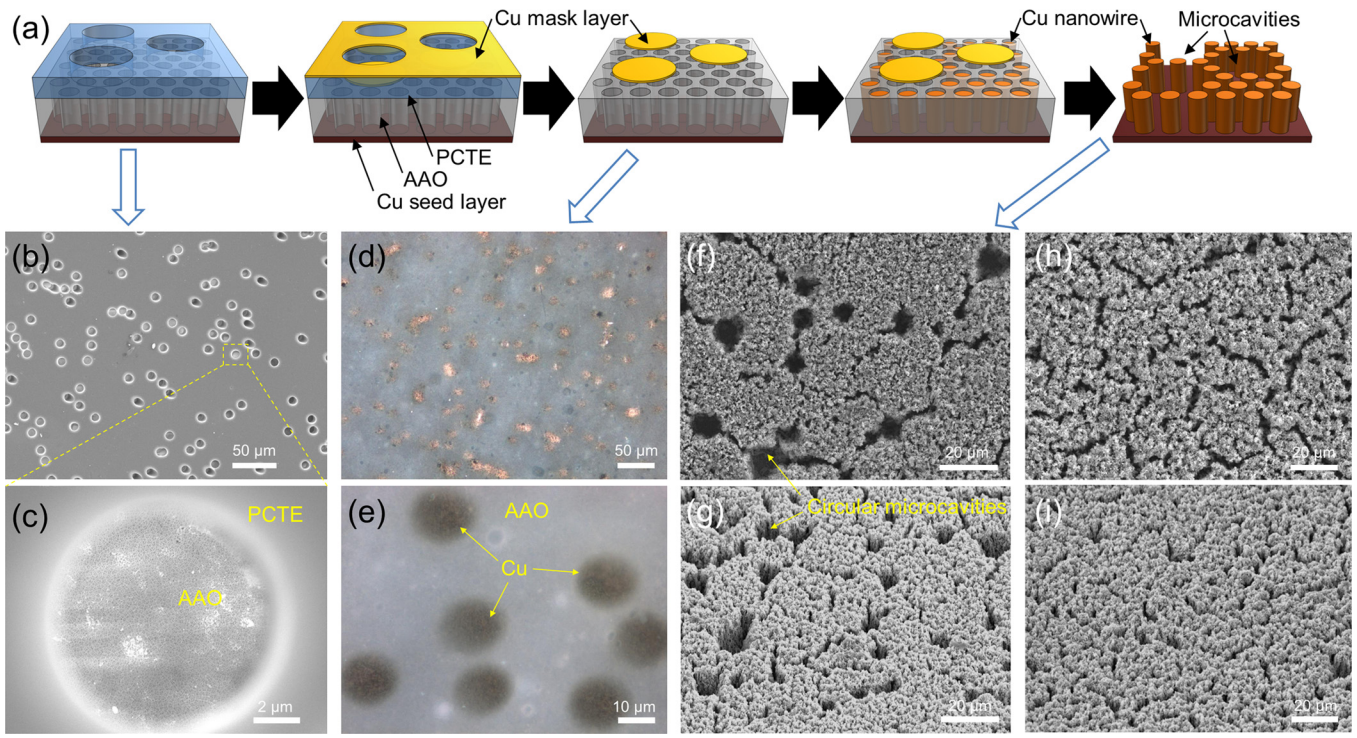

FIG. 1. Double-templated electrodeposition. (a) Schematic of the fabrication process; (b) scanning electron microscope (SEM) image of the stacked membranes and (c) magnified image of a single pore; (d),(e) optical image of the AAO template with patterned copper mask layer; (f),(g) SEM images of the electrodeposited MNHS; (h),(i) SEM image of the electrodeposited nanowire-only surface. (g) and (i) are 45° tilted images whereas others are top-view images.

features, we expect the electrodeposited MNHS surface to be beneficial to boiling heat transfer.

To verify this, we conducted pool boiling heat transfer experiment under saturated condition. Detailed procedures for boiling heat transfer experiment can be found in the supplementary information.[18] Figure 2 shows the boiling curves of the electrodeposited MNHS surface along with plain and nanowire-only surfaces. Looking into the nanowire-only results first, CHF and HTC have marked 205.8 W/cm^2 and 39150 W/m^2·K, respectively, which correspond to enhancement of over 240% and 180% compared to the plain surface, respectively. These are general findings where the similar results can be easily found in the recent literatures.[4–9] This is generally attributed to the several reasons such as increased surface area, increased nucleation sites, superhydrophilicity, capillary pumping, etc.[4,5] However, the wall superheat at ONB is 23.7 °C, which has reduced by 34% compared to the plain surface; the advancement is not as significant as CHF or HTC where the heat flux required for initiating nucleation boiling on nanowire-only surface is even higher compared to the plain surface by 54%. This is attributed to the two opposite characteristics of nanowire-only surface that affect ONB, i.e., surface wettability and surface roughness, where superhydrophilicity hinders nucleation, whereas high surface roughness promotes nucleation.[20]

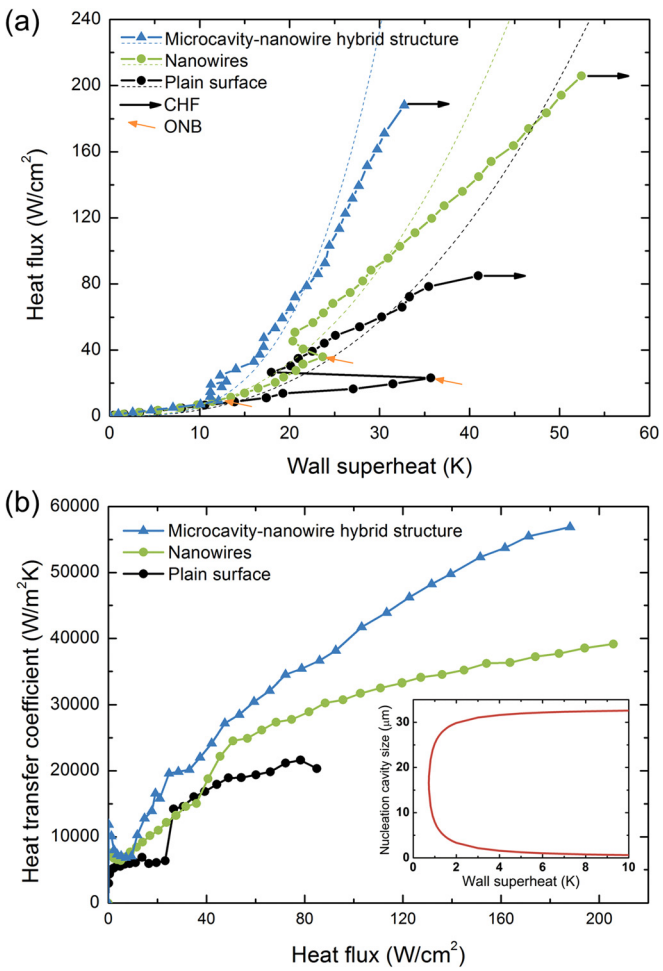

FIG. 2. Boiling performance results. Blue, green, and black colors are results for MNHS, nanowire-only, and plain surfaces, respectively. (a) Heat flux vs. wall superheat boiling curve. Symbols represent experimental results whereas dashed curves indicate theoretical fit from Eq. (1). Black and yellow arrows indicate CHF and ONB, respectively; (b) heat transfer coefficient vs. heat flux curve. The inset indicates the possible size of the nucleation cavity at a given wall superheat.

However, the most striking feature in this study is that the electrodeposited MNHS surface is shown to significantly outstand the boiling performance compared to the nanowire-only surface in terms of efficiency, i.e., HTC and ONB. Even with superhydrophilic behavior, wall superheat and heat flux required for nucleate boiling are dramatically reduced; the required wall superheat at ONB is only 12.1 °C, which has reduced by two fold compared to the nanowire-only surface. This low wall superheat eventually lead to pronounced enhancement in HTC in the entire nucleate boiling regime where the maximum HTC is obtained as 56895 W/m^2·K, which is 45% higher than nanowire-only surface.

This fast ONB on MNHS surface should be attributed to the artificially created microcavities in which these structures favor the initiation of nucleate boiling. Although the superhydrophilic surface of MNHS requires large free energy to initiate nucleate boiling,[21] large artificial microcavity is expected to further reduce the wall superheat at ONB.[22] Moreover, one can also raise a possibility of entrapment of seed bubbles at the microcavity sites that leads to low wall superheat at ONB.[23] Unlike crevice-like microcavities in nanowire-only surface where the cavities are all connected, the microcavities are individually isolated that should be more favorable to trap seed bubbles.

Also, unlike randomly formed cavities in the nanowire-only surface, these artificial microcavities exhibit predetermined geometry and location. For instance, it can be seen from the high-speed visualization in Figure 3 where the small bubble formation is randomly occurred on the nanowire-only surface (Figure 3(a)), whereas the relatively larger bubbles are uniformly formed at a certain location with uniform departure period (Figure 3(b)). From the well-known Hsu's criterion on the bubble nucleation, the size of the active nucleation cavity can be calculated as 16.6 μm at ONB (inset in Figure 2(b)).[24] This size of a cavity cannot be

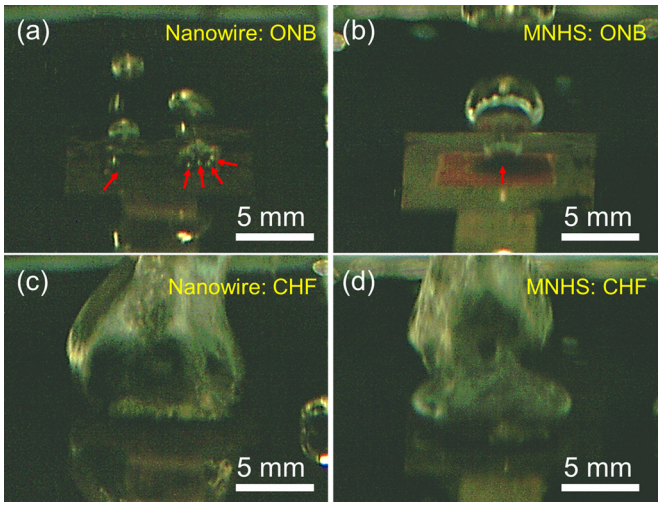

FIG. 3. Bubble visualization at a recording rate of 500 Hz. (a) Nanowire-only surface at ONB (wall heat flux = 35.9 W/cm^2); (b) MNHS surface at ONB (wall heat flux = 11.8 W/cm^2); (c) Nanowire-only surface at CHF (wall heat flux = 205.8 W/cm^2); (d) MNHS surface at CHF (wall heat flux = 188.1 W/cm^2).

easily found on the nanowire-only surface (Figures 1(h) and 1(i)) but can only be found on the MNHS surface (Figures 1(f) and 1(g)). Also, as the sizes of the artificial microcavities are observed to be ranging from approximately 5 μm to 15 μm, this geometry fall in the range of favorable cavity size that can nucleate at low wall superheat ($<10\,^{\circ}$C). Therefore, the artificial microcavities that exhibit appropriate geometry and size lead to early ONB with a minimum wall superheat, thereby dramatically increasing HTC compared to state-of-the-art nanowire surface.

To quantitatively address the enhancement of active nucleation cavities in MNHS surface, we attempted to analyze the boiling curve in relation to the active nucleation site density using the theoretical model derived by Tien.[25] The equation for the boiling curve at nucleate boiling regime can be expressed as follows:

$$q = a \cdot k \cdot \mathrm{Pr}^{0.33} \cdot N^{0.5} \cdot \Delta T, \tag{1}$$

where q is heat flux, a is a constant (61.3 for water),[25] k is thermal conductivity of water, Pr is Prandtl number of water, N is active nucleation site density, and ΔT is wall superheat. Although this equation does not render the complete hydrodynamic behavior of the boiling phenomenon, it provides an insight to the role of the nucleation cavity sites for the boiling performance. By fitting Eq. (1) to the boiling curve in Figure 2(a), we can estimate the active nucleation site density, N. Wang and Dhir[26] has experimentally shown that N is proportional to the square of q ($N \sim q^2$) and it is generally known that q follows power law with respect to wall superheat, i.e. $q \sim \Delta T^b$, where b is an unknown constant.[27] Therefore, Eq. (1) can be rewritten as follows:

$$q = a \cdot k \cdot \mathrm{Pr}^{0.33} \cdot c \cdot \Delta T^{1+b}, \tag{2}$$

where c is a constant. b can be obtained by curve-fitting the boiling curve in nucleate boiling regime where b values for the plain, nanowire, and MNHS surfaces are obtained as 1.48, 1.51, and 2.39, respectively.[18] Using these values, Eq. (1) is fitted to the boiling curve in order to obtain c. which is presented as dashed curves in Figure 2(a). Although there is a slight degree of deviation near CHF, the equation agrees well with the experimental results at nucleate boiling regime. Based on the fitting, c values for the plain, nanowire, and MNHS surfaces are obtained as 2.5, 3.5, and 0.45, respectively. From this value, we can estimate the density of active nucleation sites, N, as $6.25\Delta T^{2.19}$, $12.25\Delta T^{2.28}$, and $0.20\Delta T^{5.73}$ for the plain, nanowire, and MNHS surfaces, respectively. This leads to the fact that MNHS surface has 99.2% of more active nucleation sites compared to nanowire surface at wall superheat of 15 K, and this difference abruptly increases with increasing wall superheat; 391.8% of more active nucleation sites at wall superheat of 25 K. This clearly renders how microcavities can be favorable for nucleation. Although nanowire surface exhibits much larger nucleation sites compared to the plain surface, it is incomparable to the MNHS surface, which shows exceptional nucleation sites at higher wall superheat. This leads to pronounced enhancement of heat transfer coefficient with increasing heat flux compared to the state-of-the-art nanowire surface.

It should be noted that the electrodeposited MNHS surface exhibits a slightly lower CHF compared to the nanowire-only surface by 8.6% (188.1 W/cm^2). We attribute this to the microcavities where the surface area reduction by microcavities, which is replaced from nanowires, should not be neglected. For instance, comparing with nanowire surface, the total surface area of the MNHS surface should be exactly reduced by the porosity of PCTE, which is calculated as 8.2% from Figure 1(b). Moreover, the microcavities could possibly hinder the liquid supply near CHF. Although the microcavities can act as the nucleation sites and promote nucleation at the early stage of nucleate boiling, it should be less effective at the high heat flux region, i.e., near CHF, since the vapor bubbles are excessively grown and merged into a bulk vapor film (Figures 3(c) and 3(d)). Therefore, liquid supply is rather important in high heat flux region. Because the microcavities do not contain any nanowires, these local regions are likely to suffer from insufficient liquid supply and eventually lead to the early surface burnout. Nonetheless, the maximum HTC of MNHS surface at CHF is by far higher than the nanowire-only surface, which implies superior cooling efficiency.

In summary, we have achieved a rapid route to the fabrication of MNHS via double templating. This method provides a simple route to fabricate MNHS surface on a large area, which is very difficult to achieve by electrodeposition. We have demonstrated that this MNHS surface can be extremely efficient for boiling heat transfer where HTC and ONB were shown to excel the state-of-the-art nanowire surface. The artificially created microcavities are shown to be favorable for initiating the bubble nucleation, leading to increased heat transfer coefficient along the entire heat flux range. However, a more parametric study should be conducted in the future that regards the size and spacing of the microcavities in order to address the exact role of microcavities and find out the optimal microcavity geometries for boiling performance enhancement. Moreover, this method can be further extended to fabricate microbundles of nanowire, which is another class of MNHS, by reversing the micropattern or direct growth of nanowires with double-stacked template (first step in Figure 1(a)) that can be utilized in other applications besides boiling heat transfer such as microelectronics[16] or biotechnology.[28]

This work was supported by the National Research Foundation of Korea (NRF) grant funded by the Korea government (MEST) (No. 2012-0005727).

[1]G. Ghibaudo, H. Jaouen, and G. Kamarinos, Europhys. Lett. **2**, 209 (1986).
[2]N. A. Patankar, Soft Matter **6**, 1613 (2010).
[3]D. Coso, V. Srinivasan, M.-C. Lu, J.-Y. Chang, and A. Majumdar, J. Heat Transfer **134**, 101501 (2012).
[4]R. Chen, M.-C. Lu, V. Srinivasan, Z. Wang, H. H. Cho, and A. Majumdar, Nano Lett. **9**, 548 (2009).
[5]C. Li, Z. Wang, P.-I. Wang, Y. Peles, N. Koratkar, and G. P. Peterson, Small **4**, 1084 (2008).
[6]Z. Yao, Y.-W. Lu, and S. G. Kandlikar, Int. J. Therm. Sci. **50**, 2084 (2011).
[7]H. S. Ahn, H. J. Jo, S. H. Kang, and M. H. Kim, Appl. Phys. Lett. **98**, 071908 (2011).
[8]M.-C. Lu, R. Chen, V. Srinivasan, V. P. Carey, and A. Majumdar, Nano Lett. **54**, 5359 (2011).

[9]D. Li, G. S. Wu, W. Wang, Y. D. Wang, D. Liu, D. C. Zhang, Y. F. Chen, G. P. Peterson, and R. Yang, Nano Lett. **12**, 3385 (2012).
[10]B. S. Kim, S. Shin, S. J. Shin, K. M. Kim, and H. H. Cho, Langmuir **27**, 10148 (2011).
[11]B. S. Kim, S. Shin, S. J. Shin, K. M. Kim, and H. H. Cho, Nanoscale Res. Lett. **6**, 333 (2011).
[12]S. Shin, B. H. Kong, B. S. Kim, K. M. Kim, H. K. Cho, and H. H. Cho, Nanoscale Res. Lett. **6**, 467 (2011).
[13]S. Shin, B. S. Kim, K. M. Kim, B. H. Kong, H. K. Cho, and H. H. Cho, J. Mater. Chem. **21**, 17967 (2011).
[14]Z. Huang, N. Geyer, P. Werner, J. de Boor, and U. Gösele, Adv. Mater. **23**, 285 (2011).
[15]A. I. Hochbaum, R. Chen, R. D. Delgado, W. Liang, E. C. Garnett, M. Najarian, A. Majumdar, and P. Yang, Nature **451**, 163 (2008).
[16]A. Vlad, M. Matefi-Tempfli, V. A. Antohe, S. Faniel, N. Reckinger, B. Olbrechts, A. Crahay, V. Bayot, L. Piraux, S. Melinte, and S. Matefi-Tempfli, Small **4**, 557 (2008).
[17]S. E. Jee, P. S. Lee, B.-J. Yoon, S.-H. Jeong, and K.-H. Lee, Chem. Mater. **17**, 4049 (2005).
[18]See supplementary material at http://dx.doi.org/10.1063/1.4772539 for the experimental details on the growth of copper nanowires for MNHS, heater/sensor platform for boiling experiment, test facilities for boiling experiment, calibration of wall temperature for accurate boiling heat transfer performance, and calculation of active nucleation sites.
[19]S. M. Ghiaasiaan, *Two-Phase Flow, Boiling and Condensation in Conventional and Miniature Systems* (Cambridge University Press, New York, NY, 2008).
[20]C. H. Wang and V. K. Dhir, J. Heat Transfer **115**, 670 (1993).
[21]B. Bourdon, R. Rioboo, M. Marengo, E. Gosselin, and J. De Coninck, Langmuir **28**, 1618 (2012).
[22]B. J. Jones, J. P. McHale, and S. V. Garimella, J. Heat Transfer **131**, 121009 (2009).
[23]N. Basu, G. R. Warrier, and V. K. Dhir, J. Heat Transfer **124**, 717 (2002).
[24]Y. Y. Hsu, J. Heat Transfer **84**, 207 (1962).
[25]C. L. Tien, Int. J. Heat Mass Transfer **5**, 533 (1962).
[26]C. H. Wang and V. K. Dhir, J. Heat Transfer **115**, 659 (1993).
[27]K. Nishikawa and Y. Fujita, "Nucleate boiling heat transfer and its augmentation," in *Advances in Heat Transfer*, edited by J. P. Hartnett and T. F. Irvine (Academic, Waltham, MA, 1990), Vol. 20.
[28]B. Pokroy, S. H. Kang, L. Mahadevan, and J. Aizenberg, Science **323**, 237 (2009).